Double differential cross sections for ionization of H by 75 keV proton impact: Assessing the role of correlated wave functions

Jungang Fan(范军刚), Xiangyang Miao(苗向阳), and Xiangfu Jia(贾祥福)

Citation: Chin. Phys. B, 2020, 29 (**12**): 120301. DOI: 10.1088/1674-1056/abb7f8

Journal homepage: http://cpb.iphy.ac.cn; http://iopscience.iop.org/cpb

What follows is a list of articles you may be interested in

Exact scattering states in one-dimensional Hermitian and non-Hermitian potentials

Ruo-Lin Chai(柴若霖), Qiong-Tao Xie(谢琼涛), Xiao-Liang Liu(刘小良)

Chin. Phys. B, 2020, 29 (**9**): 090301. DOI: 10.1088/1674-1056/ab928f

Single-photon scattering controlled by an imperfect cavity

Liwei Duan(段立伟), Qing-Hu Chen(陈庆虎)

Chin. Phys. B, 2020, 29 (**7**): 070301. DOI: 10.1088/1674-1056/ab90ee

Double differential cross sections for ionization of H by 75 keV proton impact: Assessing the role of correlated wave functions

Jungang Fan(范军刚), Xiangyang Miao(苗向阳), and Xiangfu Jia(贾祥福)

Chin. Phys. B, 2020, 29 (**12**): 120301. DOI: 10.1088/1674-1056/abb7f8

Bound states resulting from interaction of the non-relativistic particles with the multiparameter potential

Ahmet Taş, Ali Havare

Chin. Phys. B, 2017, 26 (**10**): 100301. DOI: 10.1088/1674-1056/26/10/100301

Demonstration of a cold atom beam splitter on atom chip

Xiaojun Jiang(蒋小军), Xiaolin Li(李晓林), Haichao Zhang(张海潮), Yuzhu Wang(王育竹)

Chin. Phys. B, 2016, 25 (**8**): 080311. DOI: 10.1088/1674-1056/25/8/080311

RAPID COMMUNICATION

Double differential cross sections for ionization of H by 75 keV proton impact: Assessing the role of correlated wave functions*

Jungang Fan(范军刚)[1,3], Xiangyang Miao(苗向阳)[1,2,3,†], and Xiangfu Jia(贾祥福)[1,2,3,‡]

[1] *Key Laboratory of Spectral Measurement and Analysis of Shanxi Province, Shanxi Normal University, Linfen* 041004, *China*
[2] *College of Physics and Information Engineering, Shanxi Normal University, Linfen* 041004, *China*
[3] *College of Chemistry and Materials Science, Shanxi Normal University, Linfen* 041004, *China*

(Received 1 July 2020; revised manuscript received 21 August 2020; accepted manuscript online 14 September 2020)

The effect of final-state dynamic correlation is investigated for ionization of atomic hydrogen by 75-keV proton impact by analyzing double differential cross sections. The final state is represented by a continuum correlated wave (CCW-PT) function which accounts for the interaction between the projectile and the target nucleus (PT interaction). The correlated final state is nonseparable solutions of the wave equation combining the dynamics of the electron motion relative to the target and projectile, satisfying the Redmond's asymptotic conditions corresponding to long range interactions. The transition matrix is evaluated using the CCW-PT function and the undistorted initial state. Both the correlation effects and the PT interaction are analyzed by the present calculations. The convergence of the continuous correlated final state is examined carefully. Our results are compared with the absolute experimental data measured by Laforge *et al.* [*Phys. Rev. Lett.* **103**, 053201 (2009)] and Schulz *et al.* [*Phys. Rev. A* **81**, 052705 (2010)], as well as other theoretical models (especially the results of the latest non perturbation theory). We have shown that the dynamic correlation plays an important role in the ionization of atomic hydrogen by proton impact. While overall agreement between theory and the experimental data is encouraging, detailed agreement is still lacking. However, such an analysis is meaningful because it provides valuable information about the dynamical correlation and PT interaction in the CCW-PT theoretical model.

Keywords: ionization, three-body Coulomb problem, correlated wave functions, double differential cross section

PACS: 03.65.Nk, 34.80.Dp, 34.50.Fa **DOI:** 10.1088/1674-1056/abb7f8

1. Introduction

The description of three-particle Coulomb systems above their total breakup threshold constitutes a major challenge for theoretical models. Due to the long-range nature of the Coulomb forces, the motion of the three particles remains a correlated one even out to infinite inter-particle separations. In fact, for more than two mutually-interacting particles, it is well established that Schrödinger's equation is unsolvable in closed form even if the underlying force is completely understood. The theoretical models worked out for the three-body breakup apply various approximations. In the absence of an exact solution to the problem, the only way to check the accuracy and the range of the validity of the models is the comparison of their predictions with experimental data.

For ion–atom collisions, the simplest collision process is the ionization of the hydrogen by proton impact. These ionization processes are essentially a pure three-body Coulombic interacting system. This three-body system has two important advantages. First, the target atom has no passive electron(s) included in the interaction, so there is neither shielding of the nuclear charge nor any interaction between electrons. Second, the wave functions of the hydrogen atom are completely accurate. In spite of the fundamental significance of the hydrogen atom as a target, due to the well-known difficulties of the fully differential cross section (FDCS) measurements for atomic hydrogen, the majority of the ionization experiments were carried out for the hydrogen molecule,[1–3] helium,[4–7] and other heavier atoms and molecules. Although proton-hydrogen FDCS measurements are yet to be performed, experimental data on the double differential cross section ($DDCS_p$) are available.[8,9] The experiments on the hydrogen target have evoked a fresh interest in this problem.

On the theoretical side, a number of calculations have been carried out for this particular process. A major advancement in the understanding of the ionization dynamics seemed to have been accomplished at calculating the doubly differential cross sections of electrons ejected by proton impact at energies 75 keV. Schulz *et al.*[9] performed calculations using various models based on the perturbation theory. They applied the three-Coulomb wave (3C), second Born approximation–Coulomb wave (SBA-C), and continuum-distorted-wave eikonal-initial-state (CDW-EIS) models. In the CDW-EIS model, the projectile–target (PT) interaction

*Project supported by the National Natural Science Foundation of China (Grant Nos. 11974229 and 11274215).
†Corresponding author. E-mail: sxxymiao@126.com
‡Corresponding author. E-mail: jiaxf@dns.sxnu.edu.cn
© 2020 Chinese Physical Society and IOP Publishing Ltd

was accounted for both classically (CDW-EIS-CL) and semiclassically (CDW-EIS-SC). The SBA-C model was overall in good agreement with the measured data. Nevertheless, major differences between the various calculations were found. However, classical-trajectory Monte Carlo (CTMC) calculations were used by Sarkadi[10] which showed that three-body fragmentation dynamics cannot be understood purely classically. The most recent and sophisticated calculations have been performed by some authors. The coupled-pseudostate (CP) method[11] as well as more sophisticated wave packet convergent close-coupling (WP-CCC) approach[12] have been employed to calculate these cross sections. The results were found to be in good , but not perfect, agreement with the experimental data.[8,9]

Nevertheless, most of the models were believed to provide an adequate description of the collision dynamics for collision systems. The surprising observation of qualitative discrepancies between experiment and theory showed that the theory is still facing significant problems. The three-body dynamics in simple atomic systems can be considered as understood only if satisfactory agreement with experimental data is obtained consistently with a fully quantum-mechanical approach. Overall, the existing results show that three-body dynamics plays an important role in all scattering angles.[8] Accordingly, further theoretical analysis and calculations seem appropriate and interesting.

Theoretically, one of the possible problems of the theoretical models used so far within the framework of the perturbation theories is the lack of correlation in the final-state wave function.[13] The final state with correlation has been described in detail by Gasaneo *et al.* (see Refs. [14,15] and references therein), using a multivariable hypergeometric function as the approximate solution of the three-body Schrodinger equation. In other words, the final-state wave function is nonseparable solutions of the wave equation combining the dynamics of the electron motion relative to the target and projectile, satisfying the Redmond's asymptotic conditions corresponding to long range interactions. Colavecchia *et al.*[16,17] have expressed the correlated continuum wave as CCW. The correlation of the ionized electron moving in the long-range Coulomb potential of two heavy ions directly influences the essence of the dynamical process in the ionization reactions. The details of these states can be revealed by the computation of differential cross sections of electronic emission in these collisions (see Refs. [13,14,16,17] and references therein).

One of the simplest systems in which this correlation can be studied is the three-body Coulomb problem. Single ionization by ion impact can be modeled as a three-body Coulomb problem and offers the opportunity to investigate the full continuum state that describes the final state of the collision. The correlated continuum wave has been applied to the calculation of the DDCSs as a function of the emitted electron energy, under an impact parameter approximation, for $H^+ + H$, $H^+ + He$, $C^{6+} + He$, and $F^{9+} + He$ ionizing collisions by Colavecchia *et al.*[16–18] and Ciappina *et al.*[19] It has been shown that in the intermediate- to high-energy regime, the electron–ion correlation plays an important role in the single ionization of atoms by ion impact. However, Ciappina and Cravero[13] also calculated the FDCS of helium single ionization by 100 MeV/amu bare carbon projectiles using the same approximate as for the CCW function. And they found that the effect of the correlation had a slight effect on the FDCS, which could not explain these experiments. It should be noted that the PT interaction in the final state was not considered in the above mentioned calculations. In fact, it has been shown that the interaction between the projectile and the target ion, at intermediate impact energies,[8–10,20,21] has a large influence depending on the ejected electron energies and momentum transfer values. It is necessary to include the PT interaction at the level of multiple differential cross sections.[22,23] Therefore, the role of the correlation and PT interaction deserves to be studied and analyzed in more detail (see Refs. [8,9,13] and references therein).

In a recent work,[24] we proposed and developed an approach to calculate the FDCS of helium by proton impact ionization using the dynamically correlated function. The PT interaction has been accounted for not only in the CCW final state, but also in the perturbative potential. This model has been marked as CCW-PT. We have shown that the dynamic correlation plays an important role in the single ionization of helium by 75-keV proton impact. However, when the ejected electron speed is close or equal to the outgoing projectile speed, the results given by this model are unreliable (the reason is explained in the next section). At this matching velocity, the strong post-collision interaction (PCI), correlation, and PT interactions are enhanced between the ejected electron and the outgoing projectile. Significant differences between theory and experiment were found.[3,25,26] This shows that in the region of electron–projectile velocity-matching, the differential cross section is very sensitive to the details of the underlying few-body dynamics. The research of this kind of situation has aroused the great interest of more and more experimental and theoretical workers.[3,8–11,25–28] It is of theoretical interest that this collision system provides an accurate test of the theoretical description of the dynamics of the few-body dynamics.

The purpose of this work is to promote and use our CCW-PT model to investigate the role of the correlated effects and PT interaction on the double differential cross section of hydrogen atom ionized by proton impact, and to analyze whether the theoretical improvements represented by the CCW function can explain the large differences between the theory and experiment discovered so far. Therefore, we are moti-

vated to compare our CCW-PT results with the corresponding measurements[8,9] and other theoretical data, and evaluate the ability of the present model to reproduce the $\mathrm{DDCS_p}$ structure and relative magnitudes of the experiments.

The paper is set out as follows. In Section 2, the theoretical formalism and evaluation of the transition amplitude are outlined. The obtained results and their related comparisons and discussion are given in Section 3. Concluding remarks are given in Section 4. Atomic units (a.u.) are used unless otherwise stated.

2. Theoretical treatments

We deal explicitly with ionization of atomic hydrogen in the ground state by protons. The main focus of the present work is the $\mathrm{DDCS_p}$, differential in the energy of the ejected electron and the angle of the scattered projectile, measured in the experiment.[8,9] The present calculation is based on our previous techniques (see Ref. [24]), so the details of the theory are omitted here, only the basic steps and different theoretical considerations related to $\mathrm{DDCS_p}$ are summarized.

Let $\boldsymbol{K}_i$ and $\boldsymbol{K}_f$ be the initial and final wave vectors for the relative motion of the proton in the center-of-mass (c.m.) frame, and $\boldsymbol{k}_\mathrm{T}$ be the same for the ejected electron. The corresponding $\mathrm{DDCS_p}$ is given by

$$\frac{\mathrm{d}^2\sigma}{\mathrm{d}E_\mathrm{e}\,\mathrm{d}\Omega_\mathrm{P}} = (2\pi)^4\mu_\mathrm{PA}^2\frac{k_\mathrm{T}K_f}{K_i}\int|T_{fi}|^2\,\mathrm{d}\Omega_\mathrm{e}, \tag{1}$$

where $\mathrm{d}\Omega_\mathrm{P}$ and $\mathrm{d}\Omega_\mathrm{e}$ are the differential solid angles around the wave vectors $\boldsymbol{K}_f$ and $\boldsymbol{k}_\mathrm{T}$, $\mathrm{d}E_\mathrm{e}$ is the energy interval of the emitted electron, and μ_PA is the reduced mass of the proton–hydrogen system.

The main quantity in Eq. (1) is the transition matrix T_{fi} in prior form, which can be written as

$$T_{fi} = \langle\Psi_f^-|V_i|\Phi_i^+\rangle. \tag{2}$$

The undistorted initial state

$$\Phi_i^+(\boldsymbol{r}_\mathrm{T},\boldsymbol{R}_\mathrm{T}) = (2\pi)^{-3/2}\exp(\boldsymbol{K}_i\cdot\boldsymbol{R}_\mathrm{T})(1/\pi)^{1/2}\exp(-r_\mathrm{T})$$

is the product of a plane wave with momentum $\boldsymbol{K}_i$ for the incident proton and the initial target state for the hydrogen atom. $V_i = 1/R_\mathrm{T} - 1/r_\mathrm{P}$ is the initial-channel perturbation. Here, $\boldsymbol{r}_\mathrm{T}$, $\boldsymbol{r}_\mathrm{P}$, and $\boldsymbol{R}_\mathrm{T}$ are the coordinates of the electron with respect to the target core (T), the projectile (P), and the projectile relative to the atomic center of mass, respectively.

The final state Ψ_f^- is represented by the following continuum correlated wave function which accounts for the interaction between the projectile and the target nucleus (PT interaction) (see Refs. [14,15] for details):

$$\begin{aligned}\psi_f^- &= N\exp(\mathrm{i}\boldsymbol{k}_\mathrm{T}\cdot\boldsymbol{r}_\mathrm{T}+\mathrm{i}\boldsymbol{K}_f\cdot\boldsymbol{R}_\mathrm{T})\,{}_1\mathrm{F}_1(\mathrm{i}\alpha_\mathrm{PT},1,-\mathrm{i}k_\mathrm{PT}\xi_\mathrm{PT})\\ &\times\sum_{m=0}^{\infty}a_m(-\mathrm{i}k_\mathrm{T}\xi_\mathrm{T})^m\,{}_1\mathrm{F}_1(\mathrm{i}\alpha_\mathrm{T}+m,1+2m,-\mathrm{i}k_\mathrm{T}\xi_\mathrm{T})\\ &\times(-\mathrm{i}k_\mathrm{P}\xi_\mathrm{P})^m\,{}_1\mathrm{F}_1(\mathrm{i}\alpha_\mathrm{P}+m,1+2m,-\mathrm{i}k_\mathrm{P}\xi_\mathrm{P}),\end{aligned} \tag{3}$$

with

$$\begin{aligned}N &= (2\pi)^{-3}\Gamma(1-\mathrm{i}\alpha_\mathrm{PT})\Gamma(1-\mathrm{i}\alpha_\mathrm{T}-\mathrm{i}\alpha_\mathrm{P})\\ &\times\exp(-\pi[\alpha_\mathrm{PT}+\alpha_\mathrm{T}+\alpha_\mathrm{P}]/2),\end{aligned} \tag{4}$$

$$a_m = \frac{(\mathrm{i}\alpha_\mathrm{T})_m(\mathrm{i}\alpha_\mathrm{P})_m}{(m)_m(1)_{2m}m!}. \tag{5}$$

Here ${}_1\mathrm{F}_1$ and $(\alpha)_m$ are the confluent hypergeometric function and the Pochammer symbol, respectively. And $k_j\xi_j = k_jr_j + \boldsymbol{k}_j\cdot\boldsymbol{r}_j$ with $j =$ P, T, or PT. These P, T, and PT represent the projectile–electron, target–electron, and projectile–target interactions, respectively. The Sommerfeld parameters of the interaction strengths of the target–electron (T–e), projectile–electron (P–e), and projectile–target (P–T) are represented by $\alpha_\mathrm{T} = -1/k_\mathrm{T}$, $\alpha_\mathrm{P} = -1/k_\mathrm{P}$, and $\alpha_\mathrm{PT} = \mu/k_\mathrm{PT}$, respectively. $\boldsymbol{k}_\mathrm{P} \simeq \boldsymbol{k}_\mathrm{T} - \boldsymbol{K}_f/\mu = \boldsymbol{v}_\mathrm{T} - \boldsymbol{v}_f$ and $\boldsymbol{k}_\mathrm{PT} \simeq \boldsymbol{K}_f + \boldsymbol{k}_\mathrm{T}/2$ are respectively the relative momentums of the P–e and P–T subsystems. μ is the reduced mass of the projectile–target ion subsystem.

Looking closely at the final state wave (3), we can see some physical meanings it represents. First, the interaction between the heavy particles (P–T) is represented by a two-body Coulomb wave function ${}_1\mathrm{F}_1(\mathrm{i}\alpha_\mathrm{PT},1,-\mathrm{i}k_\mathrm{PT}\xi_\mathrm{PT})$ in Eq. (3). The PT interaction can be removed with an impact parameter approximation, since they do not contribute to the DDCS. However, in the present approximation, we have adopted all quantum mechanical treatments. The internuclear wave function will be kept not only in the final state, but also in the perturbative potential. Second, the series in Eq. (3) indicates the expansion of a correlated three-body function on the basis of a separable set of two-body functions, and each partial sum will give an approximation order. The correlation between the motion of the electron relative to the target nucleus and projectile is introduced approximately by the sum over all of these product states with different coefficients to Eq. (5). Third, it should be noted, besides a normalization factor, the lowest order of the final state, i.e., $m = 0$, is the well-known three-Coulomb wave function[29,30] and the correlation is included in higher orders of the series expansion. In addition, taking into account the differential properties of confluent hypergeometric functions[31]

$$\begin{aligned}&(-\mathrm{i}k_j\xi_j)^m\,{}_1\mathrm{F}_1(\mathrm{i}\alpha_j+m,1+2m,-\mathrm{i}k_j\xi_j)\\ &= \frac{(1+m)_m}{(\mathrm{i}\alpha_j)_m}\frac{\partial^m}{\partial b^m}\,{}_1\mathrm{F}_1(\mathrm{i}\alpha_j,1+m,i-\mathrm{i}bk_j\xi_j))\Big|_{b=1},\end{aligned} \tag{6}$$

so the states (6) are, apart from a plane-wave factor, the general solutions of a Schrödinger equation for a system of two particles interacting through Coulomb potentials. Therefore, the states $(-\mathrm{i}k_\mathrm{T}\xi_\mathrm{T})^m\,{}_1\mathrm{F}_1(\mathrm{i}\alpha_\mathrm{T}+m,1+2m,-\mathrm{i}k_\mathrm{T}\xi_\mathrm{T})$ and $(-\mathrm{i}k_\mathrm{P}\xi_\mathrm{P})^m\,{}_1\mathrm{F}_1(\mathrm{i}\alpha_\mathrm{P}+m,1+2m,-\mathrm{i}k_\mathrm{P}\xi_\mathrm{P})$ represent the

electron–target and electron–projectile interactions, respectively. The former represents the ionization of the hydrogen atom, and the latter is the capture of electron by the projection into a continuous state. We would like to note that each product of the states satisfies the correct asymptotic conditions in the region where all particles are far from each other.[14]

Finally, the transition matrix T_{fi} can be calculated using the final state (3) in the following way:[24]

$$T_{fi} = \lim_{M\to\infty} T_{fi}^{M} = \lim_{M\to\infty} C\hat{D}\sum_{m=0}^{M} a_m^* T_m, \tag{7}$$

with

$$\begin{aligned}\hat{D} &= \left(\frac{\partial^2}{\partial\varepsilon_1\partial\varepsilon_3} - \frac{\partial^2}{\partial\varepsilon_1\partial\varepsilon_2}\right)\Big|_{\varepsilon_1=0^+,\varepsilon_2=0^+,\varepsilon_3=0^+},\\ a_m^* &= \frac{(-\mathrm{i}\alpha_\mathrm{T})_m(-\mathrm{i}\alpha_\mathrm{P})_m}{(m)_m(1)_{2m}m!},\end{aligned} \tag{8}$$

where C is a constant, and $\hat{D}$ is a parametric differential operator. Here we have introduced the parameters ε_i $(i=1,2,3)$ for the convenience of our calculations, and take the limit $\varepsilon_i \to 0^+$ after solving the partial derivative.

The T_m has been simplified with the integral representation of the confluent hypergeometric function and the Cauchy integral theorem in our recent work.[24] However, the result is difficult for numerical integration in the present situation due to the large numerical sensitivity of the calculations when k_P becomes very small.[9] It corresponds to an ejected electron speed $\boldsymbol{v}_\mathrm{T}$ close to the projectile speed $\boldsymbol{v}_f$, that is, in the region of electron–projectile velocity-matching. The absolute value of the Sommerfeld parameter α_P can be greater than 30 a.u. in the case of larger energy loss.[3,8,9,25,26] We can see that the Sommerfild parameters α_P of these larger absolute values will lead to the fast oscillations of the integral kernel $t^{-\mathrm{i}\alpha_\mathrm{P}-1}(1-t)^{\mathrm{i}\alpha_\mathrm{P}+m}$ from the integral representation of the confluent hypergeometric function and the simplified integral is difficult to converge, even if the number of integral nodes is very large (see Eq. (27) in Ref. [24]). In this case, the confluent hypergeometric functions that need to be analytically integrated in advance should be carefully selected. In other words, integrals to be completed ahead of time should include the confluent hypergeometric functions with α_P parameter. We have adopted the following methods. After exchanging the derivative representations of formulas (12) and (13) in Ref. [24], we choose the last two confluent hypergeometric functions in Eq. (14) in Ref. [24] to be expressed in the contour integral (first simplification), and the first function in Eq. (14) in Ref. [24] is selected as the definite integral representation. Similar mathematical techniques have been successfully applied to calculate the FDCS for single ionization of helium by Au^{Q+} impact using the 3C model (see Ref. [32] and references therein).

After a large dose of mathematical manipulation, the 3D and 2D integrals (depending on the summation index m) are reached. Here only the final results are given

$$\begin{aligned}T_{m>0} &= (4\pi)^2 b_m \frac{\Gamma(1+m)}{\Gamma(-\mathrm{i}\alpha_\mathrm{T})\Gamma(1+m+\mathrm{i}\alpha_\mathrm{T})}\\ &\times \int_0^1 \mathrm{d}t\, t^{-\mathrm{i}\alpha_\mathrm{T}-1}(1-t)^{\mathrm{i}\alpha_\mathrm{T}+m}\int_0^\infty \mathrm{d}s\frac{\mathrm{i}^{-m}}{\Gamma(m)}\\ &\times \int_0^\infty \mathrm{d}\tau\,\tau^{m-1}F_m(a,b),\end{aligned} \tag{9}$$

with

$$\begin{aligned}F_m(a,b) = \frac{\partial^{3m}}{\partial a^{2m}\partial b^m}\Bigg[\frac{1}{\sigma_0}\left(\frac{\sigma_0+\sigma_1}{\sigma_0}\right)^{\mathrm{i}\alpha_\mathrm{PT}}\left(\frac{\sigma_0+\sigma_2}{\sigma_0}\right)^{\mathrm{i}\alpha_\mathrm{P}+m}\\ \times {}_2\mathrm{F}_1(-\mathrm{i}\alpha_\mathrm{PT},-\mathrm{i}\alpha_\mathrm{P}-m;1;Z)\Bigg]\Bigg|_{a=1,b=1},\end{aligned} \tag{10}$$

$$\begin{aligned}b_m &= \frac{(1+m)_m}{(-\mathrm{i}\alpha_\mathrm{P})_m}\frac{(1)_m}{(-\mathrm{i}\alpha_\mathrm{P}-m)_m}\frac{(1+m)_m}{(-\mathrm{i}\alpha_\mathrm{T})_m},\\ Z &= \frac{\sigma_1\sigma_2-\sigma_0\sigma_3}{(\sigma_0+\sigma_1)(\sigma_0+\sigma_2)}.\end{aligned} \tag{11}$$

And for $m=0$,

$$\begin{aligned}T_{m=0} = (4\pi)^2\frac{\Gamma(1)}{\Gamma(-\mathrm{i}\alpha_\mathrm{T})\Gamma(1+\mathrm{i}\alpha_\mathrm{T})}\int_0^1 \mathrm{d}t\, t^{-\mathrm{i}\alpha_\mathrm{T}-1}(1-t)^{\mathrm{i}\alpha_\mathrm{T}}\\ \times\int_0^\infty \mathrm{d}s\Bigg[\frac{1}{\sigma_0}\left(\frac{\sigma_0+\sigma_1}{\sigma_0}\right)^{\mathrm{i}\alpha_\mathrm{PT}}\left(\frac{\sigma_0+\sigma_2}{\sigma_0}\right)^{\mathrm{i}\alpha_\mathrm{P}}\\ \times {}_2\mathrm{F}_1(-\mathrm{i}\alpha_\mathrm{PT},-\mathrm{i}\alpha_\mathrm{P};1;Z)\Bigg]\Bigg|_{a=1,b=1,\tau=0}.\end{aligned} \tag{12}$$

Here, ${}_2\mathrm{F}_1$ stands for the Gaussian hypergeometric function. Readers should pay special attention to the difference between the present formulas (9)–(12) and the formulas (27) and (28) in Ref. [24]. The parameters $\sigma_0,\sigma_1,\sigma_2$, and σ_3 are

$$\begin{aligned}\sigma_0 &= \alpha_0 s^2+2\beta_0 s+\gamma_0, \quad \sigma_1 = \alpha_1 s^2+2\beta_1 s+\gamma_1,\\ \sigma_2 &= \alpha_2 s^2+2\beta_2 s+\gamma_2, \quad \sigma_3 = \alpha_3 s^2+2\beta_3 s+\gamma_3,\end{aligned} \tag{13}$$

with

$$\begin{aligned}\alpha_0 &= q^2+(\varepsilon_2+\varepsilon_3)^2+2\tau(\varepsilon_2 k_\mathrm{P}+\varepsilon_3 k_\mathrm{P}-\mathrm{i}\boldsymbol{q}\cdot\boldsymbol{k}_\mathrm{P}),\\ \alpha_1 &= 2\left[\boldsymbol{q}\cdot\boldsymbol{k}_\mathrm{PT}-\mathrm{i}(\varepsilon_2+\varepsilon_3)k_\mathrm{PT}-\mathrm{i}\tau(k_\mathrm{P}k_\mathrm{PT}+\boldsymbol{k}_\mathrm{P}\cdot\boldsymbol{k}_\mathrm{PT})\right],\\ \alpha_2 &= -2a\left[\boldsymbol{q}\cdot\boldsymbol{k}_P+\mathrm{i}(\varepsilon_2+\varepsilon_3)k_\mathrm{P}\right],\\ \alpha_3 &= -2a(\boldsymbol{k}_\mathrm{P}\cdot\boldsymbol{k}_\mathrm{PT}+k_\mathrm{P}k_\mathrm{PT}),\\ \beta_0 &= \xi_1(e_3^2+\boldsymbol{q}_2^2+\varepsilon_2^2)+\varepsilon_2(e_3^2+\xi_1^2+\boldsymbol{q}_1^2)\\ &\quad+e_3\left[\boldsymbol{q}_{12}^2+(\xi_1+\varepsilon_2)^2\right],\\ \beta_1 &= 2\xi_1(\boldsymbol{q}_2\cdot\boldsymbol{k}_\mathrm{PT}-\mathrm{i}\varepsilon_2 k_\mathrm{PT})-\mathrm{i}k_\mathrm{PT}(\xi_1^2+\boldsymbol{q}_1^2+e_3^2)\\ &\quad-2e_3\left[\boldsymbol{q}_{12}\cdot\boldsymbol{k}_\mathrm{PT}+\mathrm{i}(\xi_1+\varepsilon_2)k_\mathrm{PT}\right],\\ \beta_2 &= -2a\xi_1(\boldsymbol{q}_2\cdot\boldsymbol{k}_\mathrm{P}+\mathrm{i}e_3 k_\mathrm{P})-2a\varepsilon_2(\boldsymbol{q}_1\cdot\boldsymbol{k}_\mathrm{P}+\mathrm{i}e_3 k_\mathrm{P})\\ &\quad-\mathrm{i}ak_p\left[\boldsymbol{q}_{12}^2+(\xi_1+\varepsilon_2)^2\right],\\ \beta_3 &= -2a\xi_1\boldsymbol{k}_\mathrm{P}\cdot\boldsymbol{k}_\mathrm{PT}+2\mathrm{i}ak_\mathrm{PT}(\boldsymbol{q}_1\cdot\boldsymbol{k}_\mathrm{P}+\mathrm{i}e_3 k_\mathrm{P})\\ &\quad+2\mathrm{i}ak_p\left[\boldsymbol{q}_{12}\cdot\boldsymbol{k}_\mathrm{PT}+\mathrm{i}(\xi_1+\varepsilon_2)k_\mathrm{PT}\right],\\ \gamma_0 &= \left[\boldsymbol{q}_{12}^2+(\xi_1+\varepsilon_2)^2\right]\left[(\xi_1+e_3)^2+\boldsymbol{q}_1^2\right],\end{aligned} \tag{14}$$

$$\gamma_1 = -2\left[(\xi_1+e_3)^2+\boldsymbol{q}_1^2\right]\left[\boldsymbol{q}_{12}\cdot\boldsymbol{k}_{\rm PT}+{\rm i}(\xi_1+\varepsilon_2)k_{\rm PT}\right],$$
$$\gamma_2 = -2a\left[\boldsymbol{q}_{12}^2+(\xi_1+\varepsilon_2)^2\right]\left[\boldsymbol{q}_1\cdot\boldsymbol{k}_{\rm P}+{\rm i}(\xi_1+e_3)k_{\rm P}\right],$$
$$\gamma_3 = 4a\left[\boldsymbol{q}_1\cdot\boldsymbol{k}_{\rm P}+{\rm i}(\xi_1+e_3)k_{\rm P}\right]$$
$$\times\left[\boldsymbol{q}_{12}\cdot\boldsymbol{k}_{\rm PT}+{\rm i}(\xi_1+\varepsilon_2)k_{\rm PT}\right], \quad (16)$$

$$\boldsymbol{q}_1 = (1-bt)\boldsymbol{k}_{\rm T}-{\rm i}\tau\boldsymbol{k}_{\rm P},\ \ \boldsymbol{q}_2 = \boldsymbol{q}-{\rm i}\tau\boldsymbol{k}_{\rm P},$$
$$\boldsymbol{q}_{12} = (1-bt)\boldsymbol{k}_{\rm T}-\boldsymbol{q},\ \ \boldsymbol{q} = \boldsymbol{K}_i-\boldsymbol{K}_f,$$
$$\xi_1 = 1+\varepsilon_1-{\rm i}btk_{\rm T},\ \ e_3 = \varepsilon_3+\tau k_{\rm P}. \quad (17)$$

The detailed expressions of σ_i ($i=0$–3) can be obtained by substituting Eqs. (14)–(17) into Eq. (13). Readers can see that these σ_i are the functions of a and b. And these expressions are the linear and/or quadratic power functions of a and b. There is no difficulty in principle in completing the derivation of Eq. (10) directly. However, the consequence of the direct derivation is that the results will become extremely verbose and complex, especially for higher-order partial derivatives. For example, when $m=5$, it is the partial derivative of 15th order. The convenient way is that the derivation of Eq. (10) is done by the MATHMATICA package.

In addition, the forward difference formulas for these parameter derivatives (8) are used to ensure the convergence of the integration results.

After completing the analytical derivation of Eq. (10), the three integrals in Eq. (9) can be realized numerically by the Gauss–Legendre quadrature method for parameter t and the Gauss–Laguerre quadrature method for parameters s and τ. Convergence of the results has been tested by increasing the number of quadrate points to achieve an accuracy of 0.1%. It is necessary to sum only a few terms of the series (7).

To represent the different contributions of the terms of the sum (7) we define

$$\frac{{\rm d}^2\sigma}{{\rm d}E_{\rm e}\,{\rm d}\Omega_{\rm P}} = (2\pi)^4\mu_{\rm PA}^2\frac{K_f k_{\rm T}}{K_i}\int|T_{fi}^M|^2\,{\rm d}\Omega_{\rm e}, \quad (18)$$

which represents the DDCS$_{\rm p}$ calculated considering up to order M.

However, as observed in the laboratory, where we assume that the target is initially at rest, it is

$$\frac{{\rm d}^2\sigma^L}{{\rm d}E_{\rm e}\,{\rm d}\Omega_{\rm P}^L} = \frac{m_{\rm P}^2}{\mu_{\rm PA}^2}\frac{{\rm d}^2\sigma}{{\rm d}E_{\rm e}\,{\rm d}\Omega_{\rm P}}, \quad (19)$$

here $m_{\rm P}$ is the mass of the projectile. Whereas, under the conditions studied here, ${\rm d}E$ is essentially the same in the relative and laboratory frames, ${\rm d}\Omega_{\rm P}$ is different by a factor of $m_{\rm P}^2/\mu_{\rm PA}^2$.

In expression (18), for the final state (3) there exist several alternatives, corresponding to different proposed approximations. Therefore, we label the present calculation as CCW-PT to distinguish it from the usual CCW[13,16,17,19] theory where the PT interaction is not accounted for (referred to as the CCW-noPT). The calculations using $M=0$ are the lowest order in the transition matrix, the expression (7) reduces to the well-known 3C approximation.[29,30,33–35] The CCW-noPT calculation can be obtained by setting $\alpha_{\rm PT}=0$ in Eqs. (10) and (12), and the 2C approximation can be recovered by setting $\alpha_{\rm PT}=0$ amd $M=0$. It should be pointed out that the normalized coefficients of the 3C (2C) wave functions mentioned in the next section are all calculated by using $N_{3C}={\rm e}^{-\pi(\alpha_{\rm P}+\alpha_{\rm T}+\alpha_{\rm PT})}\Gamma(1-{\rm i}\alpha_{\rm P})\Gamma(1-{\rm i}\alpha_{\rm T})\Gamma(1-{\rm i}\alpha_{\rm PT})$ ($N_{2C}={\rm e}^{-\pi(\alpha_{\rm T}+\alpha_{\rm P})/2}\Gamma(1-{\rm i}\alpha_{\rm T})\Gamma(1-{\rm i}\alpha_{\rm P})$), at $m=0$. The calculation of the dynamic correlation involved in DDCS$_{\rm p}$ is based on this. The purpose is to examine the contribution of the correlation effect to the differential cross section more directly.

3. Results and discussion

In order to check the role of dynamic correlation in the model, we have computed the DDCS$_{\rm p}$, by Eq. (19), for 75-keV proton impact ionization of hydrogen corresponding to the experimental data of Refs. [8,9]. Figure 1 presents our results for DDCS$_{\rm p}$ as a function of the proton scattering angle θ at fixed values of the energy loss, $\Delta E=30$ eV, 40 eV, 50 eV, and 53 eV. We compare the theoretical results given by the CCW-PT (thick solid curves), 3C (dashed curves), and SBA-C (thin solid curves) calculations with the absolute experimental data from Refs. [8,9]. As mentioned above, the 3C and CCW-PT calculations are conceptually similar. In both models, the higher-order effects are accounted for in the final state, and the PT interaction has been accounted for not only in the final state, but also in the transition operator as well. They differ insofar as the CCW-PT approach, in contrast to the 3C model, accounts for dynamical correlation contributions in the final state.

It can be seen from Fig. 1 that the theoretical results describe well the main tendencies of the experimental data. However, the angular distributions and relative magnitude differences are found between the CCW-PT and 3C results. It is very encouraging to see that the CCW-PT calculations exhibit the improvement over the 3C results. Especially at $\Delta E=30$ eV, the CCW-PT model reproduces the shape of the θ dependence of the measured DDCS$_{\rm p}$ almost perfectly. We would like to explain that these improvements are due to the correlation considered in the CCW-PT approximation and not in the 3C approximation. As far as the narrowing effect is concerned, although the 3C result is improved by the CCW-PT model, it fails still to reproduce the enhancement of DDCS$_{\rm p}$ at small values of θ for the spectrum measured at $\Delta E=53$ eV. However, our CCW-PT result is in much better agreement with experiment than the SBA-C result[9] at $\Delta E=53$ eV. The agreement, in terms of magnitude, between experiment and

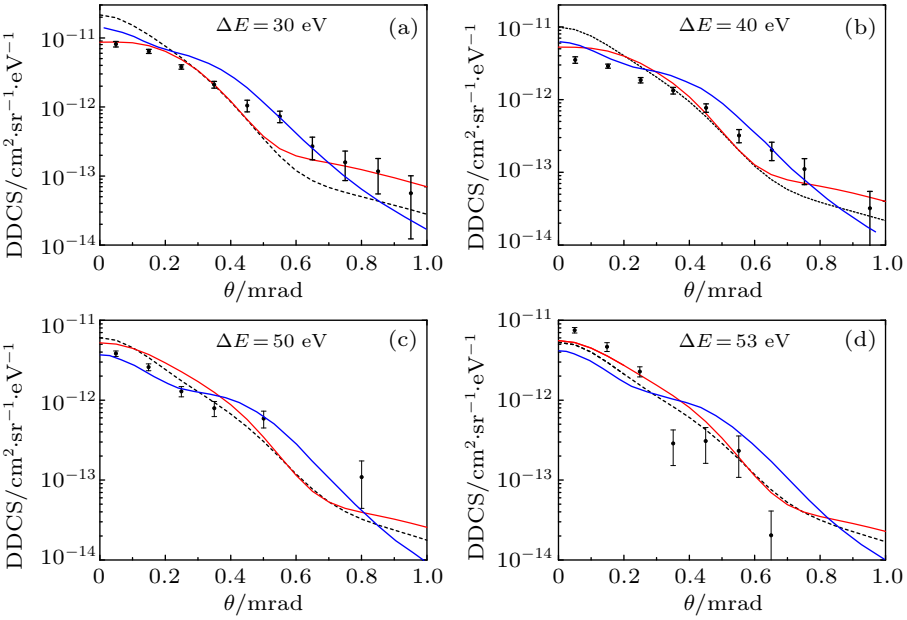

Fig. 1. Double differential cross section for ionization of the hydrogen atom by 75 keV proton impact, is plotted as a function of the projectile scattering angle for fixed energy losses as shown in the legends. The experimental data are from measurements by Laforge *et al.*[8] and Schulz *et al.*[9] The notations of the theories: thick solid curves (red), CCW-PT; dashed curves (black), 3C; thin solid curves (blue), SBA-C.[9]

the two theoretical calculations is mixed for all ΔE. In general, the present results suggest that the three-body dynamic correlation plays an important role, especially in the case of smaller energy losses. It can be seen that the changes between the cross sections displayed by the CCW-PT and 3C are relatively small for $\Delta E = 50$ eV and 53 eV. In fact, it can be seen from the following discussion that the PT interaction is more important than the dynamic correlation.

In order to test the role of the PT interaction and dynamic correlation effect in the differential cross section, we analyze the models described here in more detail by, starting from 2C (no PT interaction in the final state), successively adding dynamic correlation (denoted by CCW-noPT) and PT interaction (CCW-PT) using the respective methods of these models with goal of seeing each effect's relative importance in the $\mathrm{DDCS_p}$. All three models contain the PT interaction in operator (V_i) of the transition amplitude (2). The 2C does not deal with the PT interaction and correlation in the final state. These calculations are shown in Fig. 2. The thin solid lines represent the 2C results and dashed lines are CCW-noPT calculations. The thick solid lines still represent the CCW-PT results. As can be seen from Fig. 2, the 2C results without considering the PT interaction and dynamic correlation perform almost well in predicting experimental data, especially for low energy losses ΔE (= 30 eV, 40 eV), but for large energy losses ΔE (= 50 eV, 53 eV), it predicts $\mathrm{DDCS_p}$ much smaller than the experimental data at small scattering angles. This can be explained simply by the fact that the projectiles with a larger energy loss (corresponding to a larger electron emission speed) are more likely to approach the target nucleus and thus have more opportunities for PT interaction. So with the increase of the energy loss, the PT interaction becomes more prominent. Therefore, the 2C result is unreliable when the PT interaction is in effect. The 2C calculation here reproduces the experimental data better than the 3C model (see Fig. 1) for low energy losses ΔE (= 30 eV, 40 eV), which seems to indicate that the 3C model overestimates the importance of the PT interaction (i.e., ionization due to a binary projectile–electron interaction is kinematically possible). In fact, as can be seen from Fig. 2, the CCW-noPT calculations are significantly reduced by adding correlation to the 2C at small scattering angles. Only after adding the PT interaction, the CCW-PT results recover the experimental trend. Therefore, the ionization processes can be considered to be still dominated by the three-body dynamics.[8] At the same time, it can be seen from this figure that the dynamic correlation (CCW-noPT) has obvious effect on both sides of small scattering angles and large ones. The differences are that in small (large) scattering angles, the $\mathrm{DDCS_p}$ are decreased (enhanced) by adding correlation to 2C. However, for larger energy losses and small scattering angles, the 2C calculations are underestimated relative to these experimental data. After taking into account the dynamic correlation, although the 2C results are improved by the CCW-noPT calculation, the $\mathrm{DDCS_p}$ are still underestimated in some small angles. Only after the PT interaction is included, the CCW-PT results restore the trend of the experimental results. Therefore, for the cases of larger energy loss, the PT interaction is more important than the dynamic correlation in the whole an-

gle ranges, as shown in Fig. 2. If only the correlated effect is accounted for by the CCW-noPT, the calculated $\mathrm{DDCS_p}$ bears no resemblance to the experimental data at all in some aspects and somewhat worse than the 2C. The CCW-PT model combines the favored methods of including the long-range three-body interaction in the ionizing collision and as a result yields the best overall agreement with experiment among the models presented here.

To analyze the different effects of each of the terms in the series (7), we have computed different $\mathrm{DDCS_p}$ for ionization of hydrogen atom by 75-keV proton impact. The results are displayed in Fig. 3. The left panels show the independent $\mathrm{DDCS_p}$ with different summation indexes m $(0,1,\ldots,5)$, and the convergence results of these matrix elements for different orders M appear in the right panels. From the left panels of Fig. 3, it can be seen that the larger the index m is, the smaller the $\mathrm{DDCS_p}$ is. Starting from $m=1$, it basically reduces by one order of magnitude in turn. That is to say, with the increase of m, $\mathrm{DDCS_p}$ becomes smaller and smaller. The convergence is shown in the right panels of the figure, where the $\mathrm{DDCS_p}$ calculated with $M=0,1,\ldots,5$, i.e., the individual $\mathrm{DDCS_p}$ for $m=0,1,\cdots,5$ have been summed; each result represents the coherent sum of different orders in the transition matrix (7).

As seen from right panels of Fig. 3, besides the CCW $(M=0,1,2)$, the shape and the magnitude of each theoretical curve $(M=3,4,5)$ are approximately the same, respectively. This is further confirmation that considering up to order $M=2$ is enough to calculate the $\mathrm{DDCS_p}$ in CCW approximation. The fact clearly shows that the main correction is provided by the second order of the series $(M=2)$ and the higher orders introduce only small changes in the shape of the $\mathrm{DDCS_p}$, which can be completely ignored (also see Ref. [17] and references therein). Therefore, it is clear that the series expression (7) has an excellent numerical convergence. However, all the calculations described above are still carried out with $M=5$.

The data of Fig. 1 are shown again in Fig. 4, but this time they are compared with the corresponding WP-CCC calculations of Abdurakhmanov *et al.*[12] (performed using the coherent (coh) and incoherent (inc) combinations of the direct ionization (DI) and electron capture into continuum (ECC) amplitudes). The direct ionization and electron capture to the continuum channels are treated separately within the framework of the semiclassical two-center convergent close-coupling approach. So it leads to two ways to obtain the differential cross section (see Ref. [12] for details).

Compared with the WP-CCC coh and WP-CCC inc at $\Delta E=30$ eV and 40 eV, the former agrees better with the experiment at large scattering angle. But they are considerably higher than the measurements at small scattering angles. However, our CCW-PT results just make up for the shortcomings of the WP-CCC results.

At $\Delta E=50$ eV, the WP-CCC (including the coherent and incoherent) results are in good agreement with experiment in the entire range of scattering angles considered. Our CCW-PT results are slightly higher than the WP-CCC in the range of scattering angles $0.2<\theta<0.4$ mrad. As the energy loss is increased to 53 eV, the agreement between the WP-CCC results and the experiments appears to deteriorate. However, our CCW-PT result is in much better agreement with experiment than the WP-CCC result at $\Delta E=53$ eV.

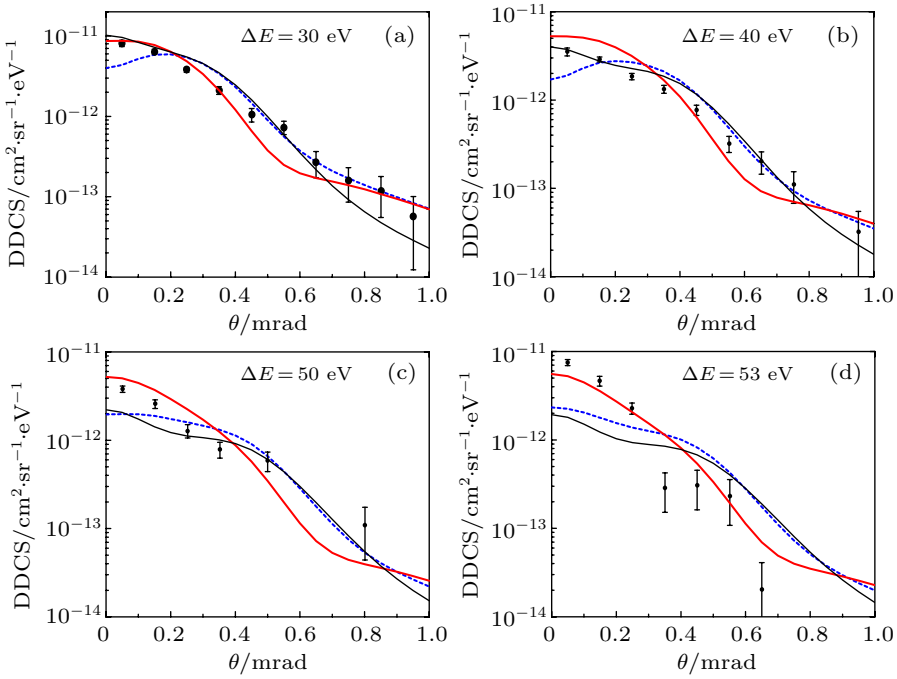

Fig. 2. Same as Fig. 1, denoted as follows: dashed curves (blue), CCW-noPT; thin solid curves (black), 2C.

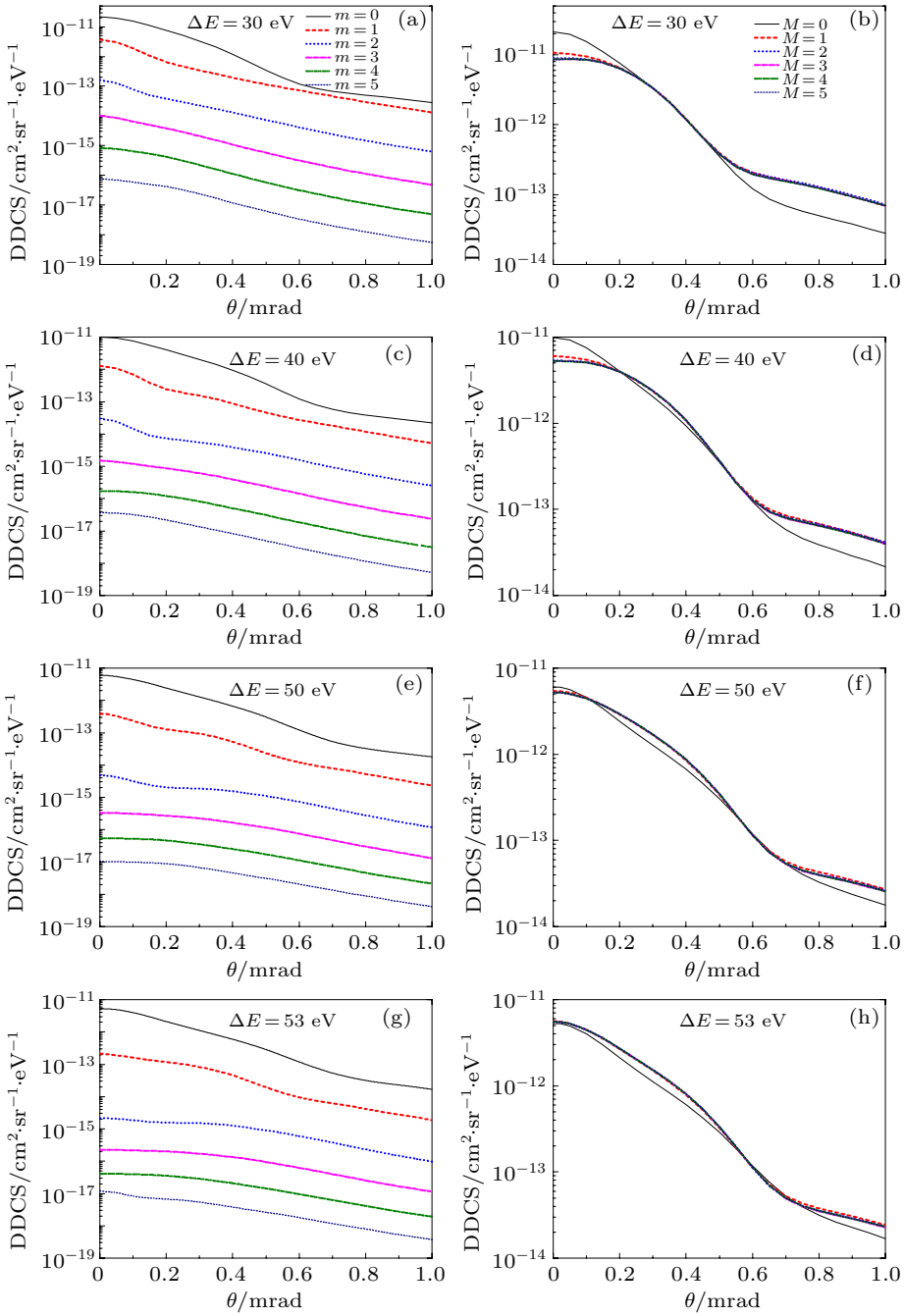

Fig. 3. The same as in Fig. 1 different Double differential cross section calculated with $m = 0, 1, 2, \ldots, 5$ (left panels), and with $M = 0, 1, 2, \ldots, 5$ (right panels). The different theoretical curves are noted in the legend.

From the comparison between these theories and experiments in Fig. 4, except for the case of $\Delta E = 50$ eV, our CCW-PT results are generally better than the WP-CCC ones. Especially at small scattering angle, the agreement between the CCW-PT and experiment is better than the WP-CCC. It is well known that the perturbative approach (CCW-PT) is more suitable for the treatment of small angle scattering systems. Since our calculation does not account for the capture channel, the comparison between experiment and theory does not allow for definite conclusions regarding its importance. The resulting discrepancies among different theories and with experimental data seem to lack any systematic pattern that could be used to track the physics underlying the observed features in the $\mathrm{DDCS_p}$ or which is missing (or not sufficiently accounted for) in theory.[7] However, WP-CCC is considered to be able to provide a sufficient description of the ionization dynamics. The surprising observation of qualitative discrepancies between experiment and theory shows that theory is still facing significant problems. The discussion above suggests that identifying the mechanisms underlying the structures in the differential cross section requires having theoretical models which yield better overall agreement with the experimental data. Our results show that the CCW-PT model is in effective range at least at 75 keV projectile energy. Of course, this model still

needs to test its applicability by comparing the calculation and experiment of more collision systems. Generally speaking, considering the relatively large value of the perturbation parameter (projectile charge to velocity ratio), the applicability of the perturbation method to this kind of collision is questionable.

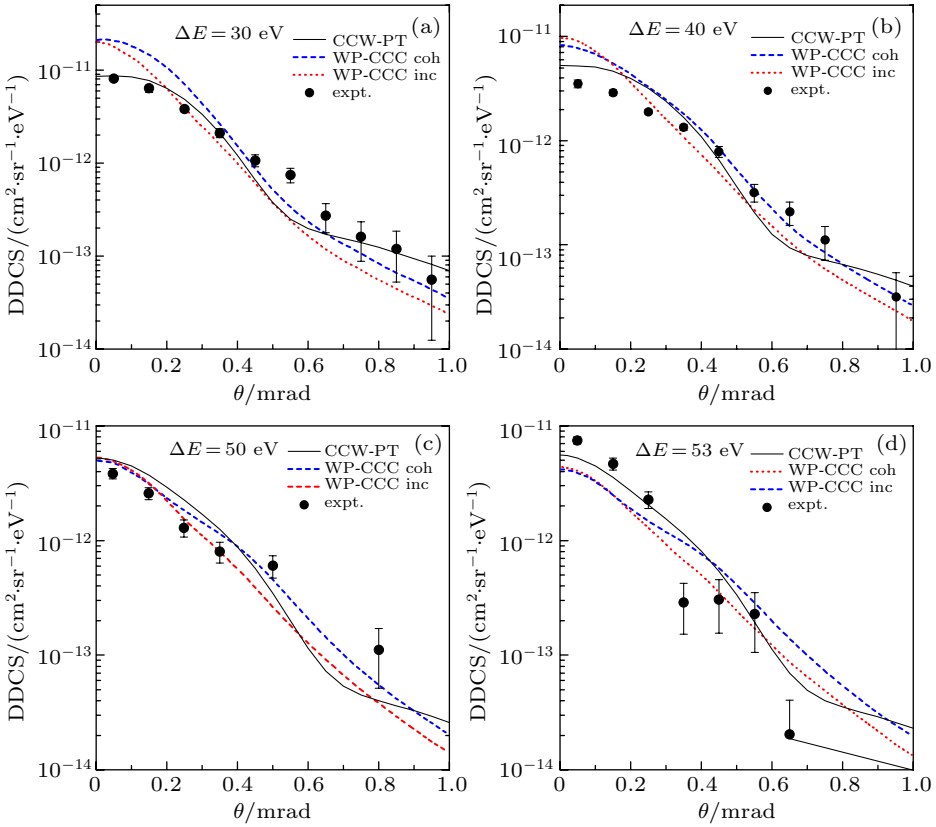

Fig. 4. Double differential cross section for 75 keV proton-impact ionization of atomic hydrogen for fixed energy losses (as indicated in the legends). The present CCW-PT results are compared with the corresponding WP-CCC calculations of Abdurakhmanov *et al.*[12] [resulting from the coherent (coh) and incoherent (inc) combinations of the direct ionization and electron capture into continuum amplitudes] and experimental measurements of Laforge *et al.*[8] and Schulz *et al.*[9]

4. Conclusions

To sum up, we have carried out CCW-PT calculations of $\mathrm{DDCS_p}$ for the ionization of atomic hydrogen by a 75-keV proton impact. We have assessed the dynamic correlation taken into account in the CCW-PT theory by comparing it with the usual 3C. Our results are also compared with those of SBA-C and WP-CCC. One of the characteristics of the dynamic correlation described by the CCW-PT is that it improves the consistency between the theoretical results of $\mathrm{DDCS_p}$ and the experimental data. The CCW-PT model is overall in good, but not perfect, agreement with the measured data. The data are compared to other theoretical calculations and the large differences between the various models show that the cross sections are quite sensitive to the details of the description of the PT interaction. For example, if only the correlated effect is accounted for (CCW-noPT), the calculated $\mathrm{DDCS_p}$ bears no resemblance to the experimental data at all in some aspects, and is somewhat worse than the 2C. On the other hand, if the PT interaction is incorporated on top of the correlation, reasonable qualitative agreement is achieved. It should also be noted that with the increase of ΔE, the PT interaction becomes more prominent. It is conceivable that the characteristics observed in the data are not only due to correlation, but also due to the PT interaction to a large extent. This is consistent with the large body of already published papers on single ionization.[4,8–10,20,21,36] It confirms that both the correlation and PT interaction which should be considered overall in our model, can take a relatively important role in the description of this collision process, especially for the large energy loss.

Compared with the experimental data and the calculated results, this difference is surprising, because $\mathrm{P+H}$ represents the simplest system, and theoretical processing is not troubled by complex many-electron states. Therefore, there are still some shortcomings in the current model in the description of ionization events. We should note that in the CCW-PT approximation, the initial and the final states are not orthogonal. And the CCW-PT methods introduce correlation in the final state but keep the initial state uncorrelated. However, Ciappina and co-workers[19] have indicated that the correlation in the initial state is necessary to describe the DDCS. The next step in this direction will be to develop some scheme where we can model an equivalent correlated initial channel[19] replacing the

undistorted Born-approximation initial one.

On the other hand, according to the WP-CCC results of Abdurakhmanov *et al.*,[12] it is shown that the electron capture to continuous state is more important than direct ionization in the collision system studied here with the increase of the energy loss, but the capture and ionization channels of the final state (3) cannot be completely separated in our treatment. In the calculation of differential cross section, our model is actually equivalent to the coupling of the two channels. To our knowledge, the calculation of capture channel is not considered in the perturbation theory dealing with this problem (see Refs. [8,9,28] for details). The WP-CCC method represents a fully nonperturbative treatment of the three-body collision system, and it can be said the most accurate theoretical results reported so far. Therefore, in order to improve the ability and reliability of perturbation model to solve practical problems, one of our tasks is to add the calculation of electron capture channel in the model. Of course, it is still a challenging work in perturbation theory. As a preliminary attempt and convenient calculation, some meaningful results may be obtained by separating 3C wave functions and treating the transition amplitudes of the direct ionization and electron capture to continuum channels separately. In fact, an ultimate test of the theoretical description of the few-body dynamics in atomic collisions would be provided by FDCS measurements for P + H ionization. Therefore, the fully differential experimental data would be very welcome. We hope that the present work can prompt further theoretical and experimental studies of the ionization process so that the role of dynamic correlation may be better understood.

References

[1] Dimopoulou C, Moshammer R, Fischer D, Höhr C, Dorn A, Fainstein P D, Crespo López Urrutia J R, Schröter C D, Kollmus H, Mann R, Hagmann S and Ullrich J 2004 *Phys. Rev. Lett.* **93** 123203

[2] Hasan A, Sharma S, Arthanayaka T P, Lamichhane B R, Remolina J, Akula S, Madison D H and Schulz M 2014 *J. Phys. B* **47** 215201

[3] Dhital M, Bastola S, Silvus A, Hasan A, Lamichhane B R, Ali E, Ciappina M F, Lomsadze R A, Cikota D, Boggs B, Madison D H and Schulz M 2019 *Phys. Rev. A* **99** 062710

[4] Schulz M, Hasan A, Maydanyuk N V, Foster M, Tooke B and Madison D H 2006 *Phys. Rev. A* **73** 062704

[5] Gassert H, Chuluunbaatar O, Waitz M, Trinter F, Kim H-K, Bauer T, Laucke A, Müller Ch, Voigtsberger J, Weller M, Rist J, Pitzer M, Zeller S, Jahnke T, Schmidt L Ph H, Williams J B, Zaytsev S A, Bulychev A A, Kouzakov K A, Schmidt-Böcking H, Dörner R, Popov Yu V and Schöffler M S 2016 *Phys. Rev. Lett.* **116** 073201

[6] Chuluunbaatar O, Kouzakov K A, Zaytsev S A, Zaytsev A S, Shablov V L, Popov Yu V and Gassert H, Waitz M, Kim H K, Bauer T and Laucke A 2019 *Phys. Rev. A* **99** 062711

[7] Dhital M, Bastola S, Silvus A, Lamichhane B R, Ali E, Ciappina M F, Lomsadze R, Hasan A, Madison D H and Schulz M 2019 *Phys. Rev. A* **100** 032707

[8] Laforge A C, Egodapitiya K N, Alexander J S, Hasan A, Ciappina M F, Khakoo M A and Schulz M 2009 *Phys. Rev. Lett.* **103** 053201

[9] Schulz M, Laforge A C, Egodapitiya K N, Alexander J S, Hasan A, Ciappina M F, Roy A C, Dey R, Samolov A and Godunov A L 2010 *Phys. Rev. A* **81** 052705

[10] Sarkadi L 2010 *Phys. Rev. A* **82** 052710

[11] Walters H R J and Whelan Colm T 2015 *Phys. Rev. A* **92** 062712

[12] Abdurakhmanov I B, Bailey J J, Kadyrov A S and Bray I 2018 *Phys. Rev. A* **97** 032707

[13] Ciappina M F and Cravero W R 2008 *Nucl. Instr. Meth. Phys. Res. B* **266** 555

[14] Gasaneo G, Colavecchia F D, Garibotti C R, Miraglia J E and Macri P 1997 *Phys. Rev. A* **55** 2809

[15] Gasaneo G, Colavecchia F D, Garibotti C R, Miraglia J E and Macri P 1997 *J. Phys. B* **30** L265

[16] Colavecchia F D, Gasaneo G and Garibotti C R 2000 *J. Phys. B* **33** L467

[17] Colavecchia F D, Gasaneo G and Garibotti C R 1998 *Phys. Rev. A* **58** 2926

[18] Colavecchia F D, Gasaneo G and Garibotti C R 1999 *Physica Scripta* **T80** 411

[19] Ciappina M F, Otranto S and Garibotti C R 2002 *Phys. Rev. A* **66** 052711

[20] Ciappina M F, Cravero W R and Schulz M 2007 *J. Phys. B* **40** 2577

[21] Duan Y H, Sun S Y and Jia X F 2015 *Europhys. Lett.* **110** 13001

[22] Li X, Ma X Y, Sun S Y and Jia X F 2012 *Chin. Phys. B* **21** 113403

[23] Lu C W, An W F, Sun S Y and Jia X F 2015 *Chin. Phys. Lett.* **32** 093401

[24] Niu X J, Sun S Y, Wang F J and Jia X F 2017 *Phys. Rev. A* **96** 022703

[25] Silvus A, Dhital M, Bastola S, Buxton J, Klok Z, Ali E, Ciappina M F, Boggs B, Cikota D, Madison D H and Schulz M 2019 *J. Phys. B* **52** 125202

[26] Hasan A, Arthanayaka T, Lamichhane B R, Sharma S, Gurung S, Remolina J, Akula S, Madison D H, Ciappina M F, Rivarola R D and Schulz M 2016 *J. Phys. B* **49** 04LT01

[27] Igarashi A and Gulyás L 2018 *J. Phys. B* **51** 035201

[28] Nassar T E I 2017 *Results in Physics* **7** 2506

[29] Garibotti C R and Miraglia J E 1980 *Phys. Rev. A* **21** 572

[30] Brauner M, Briggs J S and Klar H 1989 *J. Phys. B* **22** 2265

[31] Abramowitz M and Stegun I A (Eds.) 1964 *Handbook of Mathematical Functions with Formulas, Graphs, and Mathematical Tables*, *Appl. Math. Ser.*, Vol. 55 (Washington, DC: U.S. Government Printing Office) p. 507

[32] Sun S Y, Zhao H J and Jia X F 2018 *Europhys. Lett.* **123** 23002

[33] Jia X F, Shi Q C, Chen Z J, Chen J and Xu K Z 1997 *Phys. Rev. A* **55** 1971

[34] Bandyopadhyayt A, Roy K, Mandal P and Sil N C 1994 *J. Phys. B* **27** 4337

[35] Ma X Y, Li X, Sun S Y and Jia X F 2012 *Europhys. Lett.* **98** 53001

[36] Ciappina M F and Cravero W R 2006 *J. Phys. B* **39** 2183